Composites: Part B 43 (2012) 1749–1755

Contents lists available at SciVerse ScienceDirect

Composites: Part B

journal homepage: www.elsevier.com/locate/compositesb

Hybrid truss concepts for carbon fiber composite pyramidal lattice structures

Sha Yin [a], Linzhi Wu [a,*], Li Ma [a], Steven Nutt [b]

[a] Center for Composite Materials, Harbin Institute of Technology, Harbin 150001, China
[b] Department of Chemical Engineering and Materials Science, University of Southern California, Los Angeles, CA 90089-0241, USA

ARTICLE INFO

Article history:
Received 7 August 2011
Received in revised form 16 November 2011
Accepted 2 January 2012
Available online 10 January 2012

Keywords:
A. Carbon fiber
A. Hybrid
B. Mechanical properties
Composite lattice

ABSTRACT

A novel hybrid truss construction concept is presented that incorporates a second-phase core material into trusses of carbon fiber (CF) composite pyramidal lattice (CPL) structures. Embedded core materials of wood and silicone rubber are selected for trial structures. Hybrid CPL structures were fabricated using a hot press molding approach and out-of-plane compression tests were performed to investigate properties. For prototype wood–core truss CPL, structural efficiencies increased comparing with solid truss CPL, while energy absorption capability was enhanced for rubber–core truss CPL. Employing the hybrid truss construction, the density-specific performance space of CF composite lattice structures can be expanded, and desired functional potential can be realized by judicious selection of core materials while simultaneously retaining structural properties.

1. Introduction

Lattice structures exhibit promise for lightweight structural applications and multifunctional materials [1–3]. When multiple functions are involved, a truss core material or "gap phase" is typically employed to introduce additional functionality, such as heat transfer [4] or impact protection [5]. Selection of truss topology or parent material can be used to alter the properties of such materials [6]. Early studies reported the effects of geometric variants of metallic lattices, such as octet-truss [7], Kagome lattice [8] and pyramidal lattice [9]. Subsequent investigations described microtruss structures fabricated using a novel waveguide approach [10,11] or electrodeposition [12]. Recent reports have shown that hybrid designs employing carbon fiber composites and optimized lattice topology can yield lattice structures with superior mechanical performance than their metallic counterparts. These new engineering materials simultaneously increase design space and fill gaps in the material property space [6]. Multiple fabrication methods [13–19] have been developed for composite lattice cores and associated sandwich structures, moving the approach closer to deployment in engineering applications.

In this study, we employ a new hybrid truss design for lattice structures intended for sandwich structures. The hybrid truss elements consist of a carbon fiber (CF) composite shell surrounding a second-phase core material. The intent is to provide a strengthening strategy for traditional solid truss composite lattice structures of ultra-low density, and simultaneously demonstrate the additional functional potential by incorporating selected core materials into the trusses. The outline of this paper is as follows. In Section 2, the novel hybrid truss concept is presented and explained, followed by a description of the fabrication method. In Section 3, the out-of-plane compression behavior of prototype structures is presented. A simple mechanical analysis and parametric study is presented to demonstrate the performance and the increased design space.

2. Construction concept and fabrication approach

2.1. Construction concept

Fig. 1 illustrates two types of truss constructions, defined as unitary truss and hybrid truss, respectively. The unitary truss consists solely of carbon fiber composites, such as solid truss (Fig. 1a) and hollow truss (Fig. 1b), while the hybrid truss (Fig. 1c) is composed of a CF composite shell surrounding a second-phase embedded core material. The hybrid truss construction is employed to produce composite pyramidal lattice (CPL) structures, as shown in Fig. 1d.

In the present study, two kinds of core materials were selected for hybrid trusses: lightweight wood and super-elastic silicone rubber. The wood–core truss lattice structures are expected to yield exceptional resistance to elastic buckling, an important feature of ultra-lightweight solid truss lattice structures, where truss buckling generally controls failure. In contrast, the rubber–core trusses are expected to enhance energy absorption capacity due to the elasticity of the rubber core.

* Corresponding author. Tel.: +86 451 86412549; fax: +86 451 86402379.
E-mail address: wlz@hit.edu.cn (L. Wu).

1359-8368/$ - see front matter © 2012 Elsevier Ltd. All rights reserved.
doi:10.1016/j.compositesb.2012.01.033

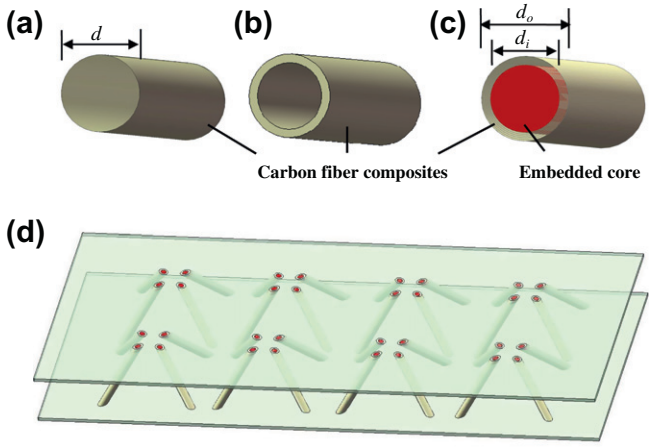

Fig. 1. Schematic illustrations: (a) Solid truss; (b) hollow truss; (c) hybrid truss; (d) pyramidal lattice sandwich structure with hybrid trusses.

2.2. Fabrication approach

Fabrication of the composite pyramidal lattice (CPL) sandwich structures is based on a hot press molding approach. The method, which employs assembled steel molds, was originally used to produce solid truss composite pyramidal lattice (CPL) materials for sandwich structures [15]. The process has been adapted here for production of hybrid truss lattice structures. First, unidirectional CF/epoxy prepregs (T700/3234) were laid up and wrapped around the core rods to form hybrid trusses. The stacking sequence was $[0]_2$ for wood–core trusses and $[0_2/90_2]$ for rubber–core trusses. Here, 0 represents the CF-truss axis angle, and 90 is the circumferential direction. Such hybrid trusses were inserted into the cylindrical cavities of assembled molds, as shown in Fig. 2a. Then, plies of CF prepreg were perforated such that the holes matched the truss positions. The perforated prepreg plies were laid over the hybrid trusses, and the CF composite shells at the ends of each hybrid truss were peeled from the rods and subsequently embedded between two plies of the perforated prepreg (Fig. 2b). Next, the excess silicone rubber in each hybrid truss was removed, and unidirectional prepreg plies were overlaid and stacked to produce face sheets on the top and bottom surfaces of the steel molds. Finally, the assembly was cured in a hot press at 125 °C and 0.5 MPa for 2 h. After removing the molds, CF CPL sandwich structures with hybrid trusses were obtained. Fig. 3 shows the fabricated CPL structures with wood–core trusses and rubber–core trusses, respectively.

2.3. Relative density

The representative unit cell of CPL structures with hybrid trusses is shown in Fig. 4. The relative density $\bar{\rho}$, defined as the ratio of the density of the pyramidal core to that of the parent carbon fiber composite ρ_{cf}, is given by

$$\bar{\rho} = \frac{\pi\left(d_o^2 - d_i^2\right) + \pi d_i^2 \rho_i/\rho_{cf}}{\sin\omega\left(\sqrt{2}l_1\cos\omega + 2l_2\right)^2} = \bar{\rho}_{cf} + \bar{\rho}_i \tag{1}$$

where d_o is the outer diameter of hybrid trusses, d_i and ρ_i are the diameter and density of the embedded core, l_1 is the hybrid truss length, ω is the inclination angle between the truss members and the base of the unit cell, and l_2 represents the side length of the square at the top of a pyramidal core; $\bar{\rho}_{cf}$ and $\bar{\rho}_i$ are the corresponding proportions of relative density occupied by the carbon fiber tube and the embedded core, respectively.

Here, $\rho_{cf} = 1.55\ \mathrm{Mg/m^3}$, so for the wood–core truss structures, $\rho_i/\rho_{cf} \approx 1/4$, while for the rubber–core truss structures, $\rho_i/\rho_{cf} \approx 1$.

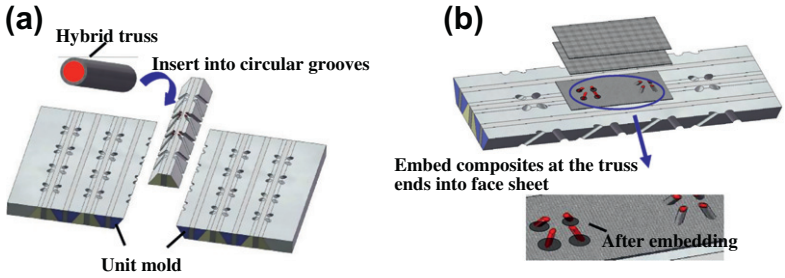

Fig. 2. Illustration of the fabrication approach for CF composite pyramidal lattice core sandwich structures with hybrid trusses.

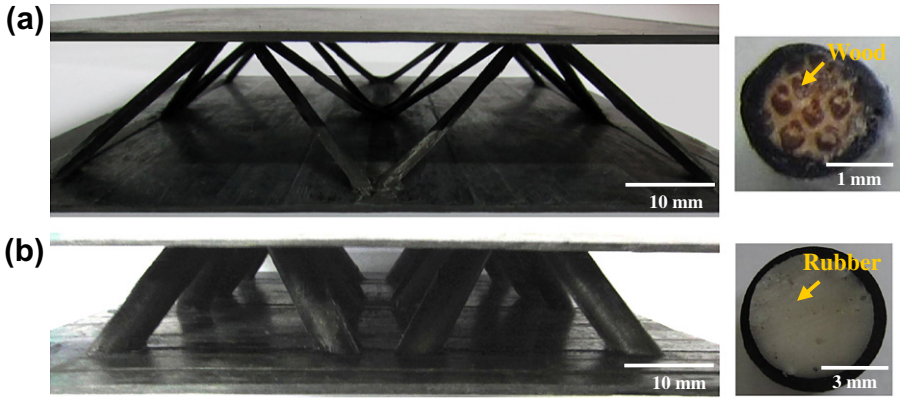

Fig. 3. (a) Wood–core truss (b) silicone rubber–core truss and their corresponding carbon fiber composite pyramidal lattice structures.

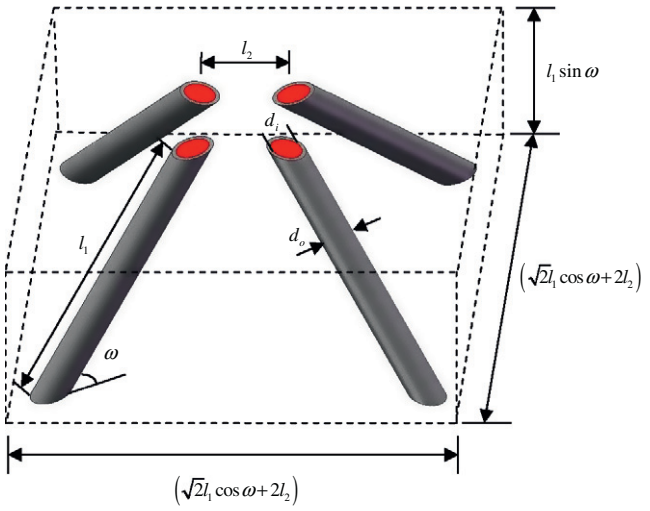

Fig. 4. Unit cell of a pyramidal lattice structure with hybrid trusses.

Four kinds of samples were fabricated and two sets of comparison were carried out to illustrate the construction concept, including CPL sandwich structures with (1) wood–core trusses and solid trusses, (2) rubber–core trusses and hollow trusses. The geometries are summarized in Table 1. Note that solid truss CPL structures were fabricated in the same molds as the wood–core truss counterparts with the same core geometries, denoted with a subscript "*u*" in the following sections. Meanwhile, CPL structures with hollow trusses were fabricated in the same molds as those with rubber–core trusses.

3. Out-of-plane compression experiments

The mechanical properties of the hybrid truss CPL structures were explored through nominal compression tests. These structures were tested in compression with a displacement rate of 0.5 mm/min at room temperature using a screw-driven testing machine (INSTRON 5569) following ASTM C365/C 364M-05 [20]. At least two specimens are tested for each type to gauge the level of the experimental scatter.

3.1. Wood–core truss CF CPL

CPL structures with wood–core trusses and those with solid trusses were tested in one group for comparison. The representative through-thickness nominal compressive stress–strain response for these two CPL structures is shown in Fig. 5a. The curve of the wood–core truss lattice structure exhibits characteristics similar to those of counterpart CPL structures featuring solid truss construction of CF composites. After an initial linear response, a peak stress is observed at a relatively small strain (~0.02–0.05), which coincides with failure of trusses. As loading continues, the stress decreases, accompanied by further crushing, and core "softening" behavior is observed. The governing failure mode is tube wall fracture for the wood–core truss structure, while elastic buckling is the characteristic failure mode for the slender solid truss counterpart. The compressive modulus and peak strength of the wood–core truss structure are lower than those of the solid truss structure, and this is attributed to the much lower volume fraction of carbon fiber composite in the truss members. The mechanical properties of the unidirectional CF rods were obtained by the compression test of the single truss sandwich developed in the published paper [14], yielding values of E_{cf} = 24.5 GPa and σ_{cf} = 326 MPa, which will be used for prediction in the following section.

3.2. Rubber–core truss CF CPL

Rubber–core truss CPL structures incorporating circumferentially fibers (Type A) and those with only 0 fibers (Type B) were tested and compared with the CPL structures without filling rubber. The hollow truss structures were similarly constructed and fabricated using the same stacking sequences as those in the rubber–core structures of Type A. The compressive stress–strain curves are shown in Fig. 6a. The compressive response of solid truss CPL, and that of bulk silicone rubber which exhibits typical elastomeric behavior are also included for reference. The

Table 1
Summary of the geometries for composite pyramidal lattice structures with different kinds of trusses.

Truss type	d_o (mm)	d_i (mm)	d (mm)	l_1 (mm)	ω (°)	l_2 (mm)
Solid truss	–	–	2	34.6	35.26	3
Wood–core truss	2	1.5	–	34.6	35.26	3
Rubber–core truss	6	5.4	–	19.8	45	15
Hollow truss	6	5.4	–	19.8	45	15

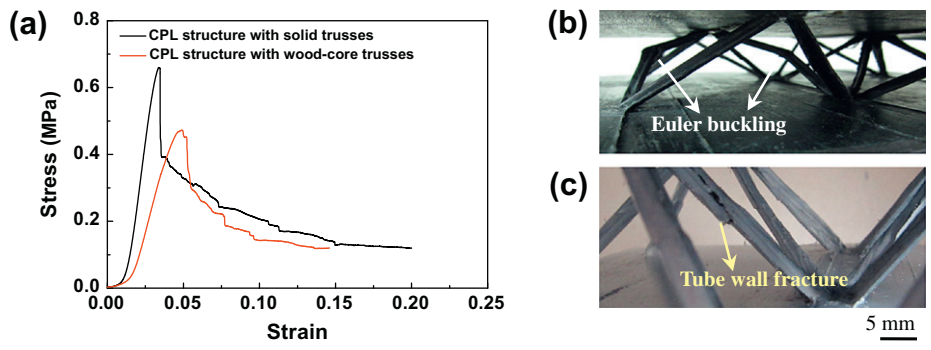

Fig. 5. (a) Compressive stress–strain responses for CF CPL structures with wood–core trusses and solid trusses; (b) failure mode of solid truss CPL; (c) failure mode of wood–core truss CPL.

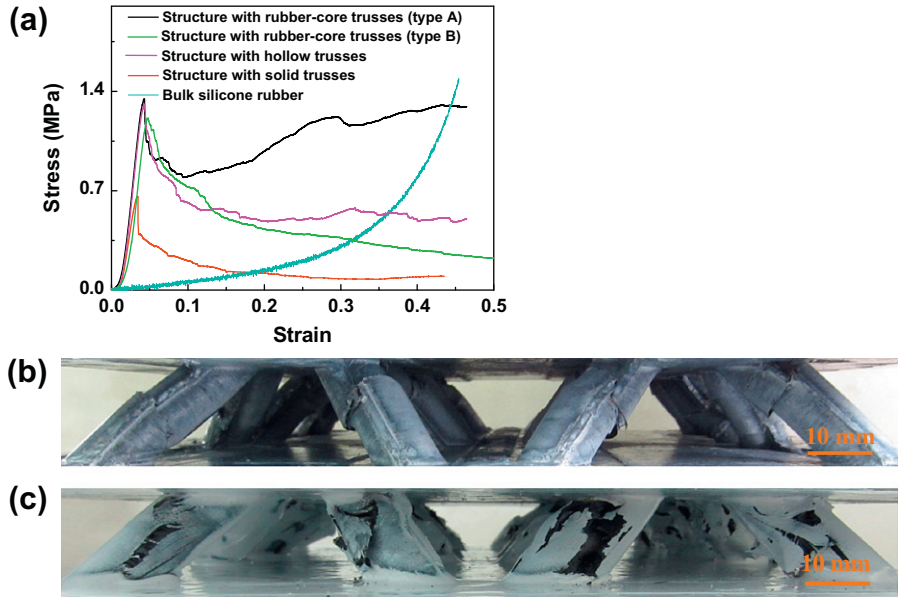

Fig. 6. (a) Compressive stress–strain curves of CF CPL structures with rubber–core trusses compared with those without filling rubber; (b) the corresponding failure mode for CPL structures with rubber–core trusses (Type A); (c) failure mode of rubber–core truss CPL structure with only 0 fibers uniaxially lying along the truss member (Type B).

compressive behavior of the CPL sandwich structure with rubber–core trusses after incorporating circumferentially fibers (Type A) differs from that of the corresponding structure of Type B or that without filling rubber. Initially, the response is linear elastic and resembles the behavior of CPL structures composed of CF. For CPL structures of Type A and that of hollow truss CPL structures, a peak strength is reached, followed by a stress drop associated with tube wall failure as shown in Fig. 6b. Moreover, the compressive modulus and peak strength values for these two kinds of structures are comparable, indicating that the rubber contributes little to the stiffness and strength at this stage. Subsequently, unlike the long stress plateau shown by hollow truss lattice structures (where the stress gradually decreased with increasing strain), a gradual strain hardening period appeared in the stress plateau for the hybrid truss CPL structure. During this period further crushing of the structures occurred, starting at a strain of ~0.1. The constrained rubber inside the truss resists the deformation and buckling of the structures, leading to the strain hardening region (the strain from 0.1 to about 0.5). The response of rubber–core truss CPL structure of Type B, which failed by fiber splitting of composite tube, is similar to that of hollow truss and no strain hardening period appeared.

In summary, the measured strength are within 7% scatter which is not uncommon in structures made from carbon fiber composites. The mechanical properties of those parent materials are sensitive to the environment and small imperfection might be introduced during the manufacturing process.

4. Analysis

4.1. Out-of-plane compression

The hybrid truss construction provides a strategy for ultra lightweight composite lattice structures with slender trusses, where Euler buckling controls failure. Thus, the bending contribution to stiffness and strength will not be considered here. The effective compressive properties of the two prototype structures, featuring either wood–core trusses or silicone rubber–core trusses, can be deduced by analyzing the deformation of a single hybrid truss [14]. We will assume that truss ends have clamped boundary conditions.

4.1.1. Compressive elastic modulus

The nominal compressive modulus of CPL structures can be expressed as

$$E_c = E_{cf}\bar{\rho}_{cf}\sin^4\omega \tag{2}$$

where E_{cf} is the elastic modulus of the parent carbon fiber composites (T700/3234). The compressive modulus of a CPL structure depends on the proportion of relative density occupied by carbon fiber composites.

4.1.2. Peak compressive stress

With the simplifying assumptions suggested by Budiansky [21], the core can stabilize the tube walls against wrinkling. The contribution of the core to the bending stiffness of the hybrid truss and the contribution of the compressive stress in the core to the total applied load are neglected. Euler macro buckling of hybrid truss and tube wall fracture will be considered as two competitive failure modes. Accordingly, the failure stress of hybrid trusses σ_c will be expressed as

$$\sigma_c = \begin{cases} \frac{\pi^2}{4}\frac{\left(d_o^2+d_i^2\right)}{l_1^2}E_{cf} & \left(d_o^2+d_i^2\right) < \left(4l_1^2\sigma_{cf}\right)\left(\pi^2 E_{cf}\right)^{-1} \\ \sigma_{cf} & \text{otherwise} \end{cases} \tag{3}$$

where σ_{cf} is the fracture strength of carbon fiber rods, often obtained by direct measurement rather than by the predictions of micromechanical models. The peak compressive strength σ_p of a composite pyramidal core with hybrid trusses can be deduced as

$$\sigma_p = \sigma_c\bar{\rho}_{cf}\sin^2\omega \tag{4}$$

To access the effectiveness of the strengthening strategy, the measured compressive peak strength σ_p of hybrid truss CF CPL structures are shown in Table 2 and compared with similar structures with slender solid trusses. Mechanical properties of hollow truss CPL structures are also included for the comparison of energy

Table 2
The compressive strength of CPL structures with different kinds of trusses.

Truss type	$\bar{\rho}$ (%)	Stacking sequence	Failure mode	Strength (MPa)		Specific strength (MPa/(Mg/m^3))
				Exp.	Ana.	Exp.
Solid truss	1.03	–	E	0.66	0.693	41.34
Wood–core truss	0.585	[wood/0_2]	F	0.447	0.478	49.30
Rubber–core truss (Type A)	6.45	[rubber/0_2/90_2]	F	1.35	–	13.5
Rubber–core truss (Type B)	6.45	[rubber/0_4]	S	1.21	1.338	12.1
Hollow truss	1.23	[0_2/90_2]	F	1.31	–	68.71

F = tube wall fracture; E = Euler buckling; S = splitting; Exp. = experimental; Ana. = analytical.

absorption capacity in Section 4.3. The analytical model for the CPL structures with stocky hollow trusses has been discussed in the published paper [14].

4.2. Structural efficiency

The specific properties of the CPL structures with hybrid trusses will be considered by comparison to those of solid truss CPL structures of low relative density (generally $\bar{\rho} < 5\%$), which often fail by Euler buckling. Although the embedded core is assumed to contribute little to the compressive behavior of these hybrid truss CPL structures, the Euler buckling resistance of the hybrid lattice structure is greatly enhanced relative to the solid counterpart. Note that there is a weight penalty associated with the core materials, which will affect specific properties as discussed below.

4.2.1. Compressive specific modulus

The specific modulus $(E_c/(\bar{\rho}\rho_{cf}))$ of a CPL structure with hybrid trusses can be expressed as $E_c/\bar{\rho}\rho_{cf} = \xi E_{cf}\sin^4\omega/\rho_{cf}$, where $\xi = \left(1 + \frac{d_i^2}{d_o^2 - d_i^2}\frac{\rho_i}{\rho_{cf}}\right)^{-1}$ is a non-dimensional coefficient related to the inner diameter and density of the core material, which can be used to compare specific modulus of CPL with different trusses. For solid truss CPL structures ($d_i = 0$), $\xi_s = 1$; while for hybrid truss CPL structures, $\xi_h < 1$. Therefore, the specific modulus of a hybrid truss lattice will be less than that of a solid truss lattice (Fig. 7a and c).

4.2.2. Peak specific strength

The peak specific strength of a hybrid truss CPL structure $(\sigma_{pk}/(\bar{\rho}\rho_{cf}))$ is given by dividing Eq. (4) by the density of the pyramidal lattice, giving

$$\frac{\sigma_{pk}}{\bar{\rho}\rho_{cf}} = \begin{cases} 16\pi^2\frac{E_{cf}}{\rho_{cf}}\sin^2\omega\cdot\eta & d_o^2 + d_i^2 < \left(4l_1^2\sigma_{cf}\right)\left(\pi^2 E_{cf}\right)^{-1} \\ \frac{\sigma_{cf}}{\rho_{cf}}\sin^2\omega\cdot\xi & \text{otherwise} \end{cases} \quad (5)$$

which yields non-dimensional coefficients ξ and η. ξ here is set to evaluate the variation of peak specific strength when the structures fail by tube wall fracture, while $\eta = (64l_1^2)^{-1}\left(d_o^4 - d_i^4\right)\left[\left(d_o^2 - d_i^2\right) + d_i^2\rho_i/\rho_{cf}\right]^{-1}$ is used to evaluate the variation of Euler buckling specific strength. For CPL structures with slender solid truss ($d_i = 0$), the failure is always controlled by Euler buckling, which gives $\eta_s = \left(64l_{1s}^2\right)^{-1}d^2$.

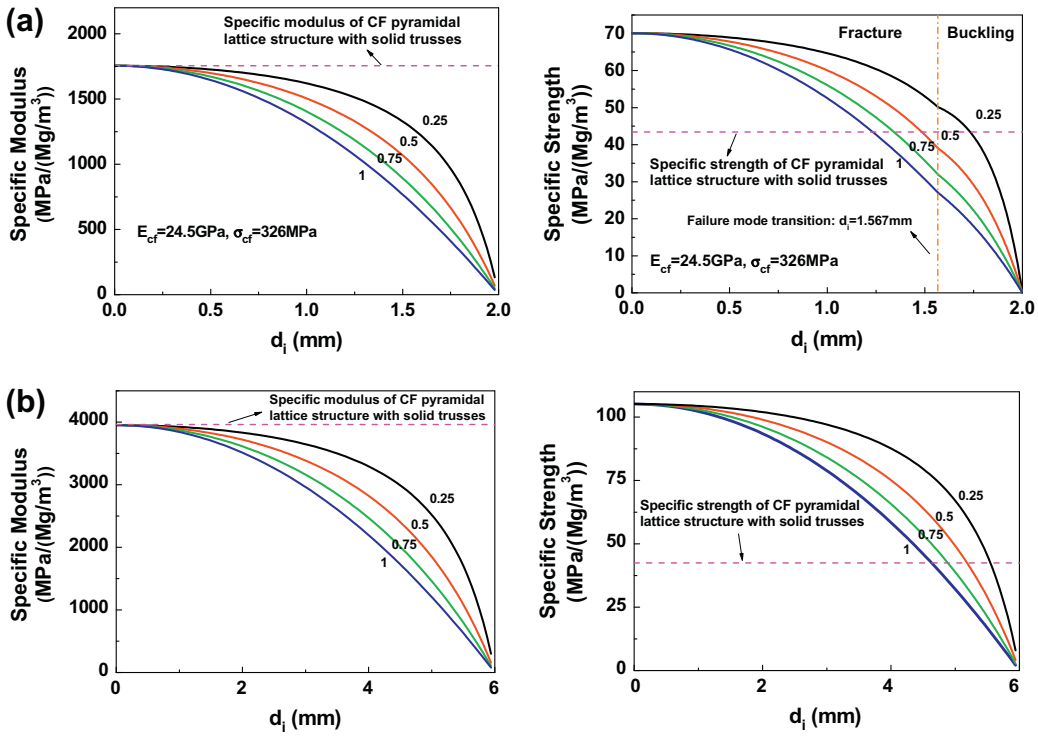

Fig. 7. (a) Specific modulus and strength for CPL structures with high aspect ratio; (b) specific modulus and strength for CPL structures with low aspect ratio trusses plotted as a function of the diameter of the embedded core for different core densities.

To ensure that the specific strength of a hybrid truss CPL structure exceeds that of a counterpart solid truss CPL structure, the density of the embedded core materials is restricted as shown below

$$\rho_i < \begin{cases} \left[1 + \frac{l_{1s}^2\left(d_o^4 - d_i^4\right)}{l_1^2 d^2 d_i^2} - \frac{d_o^2}{d_i^2}\right]\rho_{cf} & \left(d_o^2 + d_i^2\right) < \left(4l_1^2\sigma_{cf}\right)\left(\pi^2 E_{cf}\right)^{-1} \\ \left(\frac{4l_{1s}^2}{\pi^2 d^2}\frac{\sigma_{cf}}{E_{cf}} - 1\right)\left(\frac{d_o^2}{d_i^2} - 1\right)\rho_{cf} & \text{otherwise} \end{cases} \tag{6}$$

The inequality indicates that for a specific pyramidal core geometry, the specific strength can be increased by the selection of the failure mode (controlled by d_i for slender trusses) and the density of the embedded core material ρ_i. Applying this analysis to the slender geometries in the experimental section, the restriction predicted by Eq. (6) is $\rho_i < 0.36\rho_{cf}$ with $d_i = 1.5$ mm, which can be satisfied by employing wood ($\rho_i/\rho_{cf} \approx 1/4$) cores to improve the structural efficiency (defined as load-carrying capacity per unit mass).

The specific modulus and strength for these composite pyramidal lattice structures with both high and low aspect ratio trusses (shown in Table 1) is plotted as a function of the diameter of the embedded core for different ρ_i/ρ_{cf} ranging from 0.25 to 1.0 Mg/m^3 as shown in Fig. 7. The specific modulus and strength decrease with increasing d_i or ρ_i/ρ_{cf}, whether the failure mode is Euler buckling or tube wall fracture. As shown in Fig. 7, both lightweight wood ($\rho_i/\rho_{cf} \approx 1/4$) and heavier silicone rubber cores ($\rho_i/\rho_{cf} \approx 1$) can be used to improve specific strength of CPL structures with slender solid trusses, albeit with different selection of d_i.

The measured specific strength of wood–core truss CPL structures in the present study increased by >19% (Table 2); while rubber–core truss CPL structures decreased. The increase is attributed to the transition of failure mode from Euler buckling for solid truss CPL structures, and to the relatively low weight penalty of the wood core material. The findings indicate that the hybrid truss construction can be employed to expand the density-specific performance space of lattice materials.

4.3. Multifunctional potential

The strain energy absorbed during compression up to the onset of densification can be used as a figure of merit to compare different cellular structures for impact energy absorption [22]. The energy absorption capacity per unit volume, W_v, is obtained from the area under the stress–strain curve. In out-of-plane compression, the strain-hardening regime observed for silicone rubber–core truss lattice structures (Type A in Fig. 6a) enhances energy absorption. The structural response of a rubber–core truss CPL structure $\sigma(\varepsilon)$, is the combination of the compressive stress–strain response of a hollow truss composite pyramidal core $\sigma_{ho}(\varepsilon)$, and that of the silicone rubber rod $\sigma_{rubber}(\varepsilon)$ inside the truss. The combined response can be expressed as

$$\sigma(\varepsilon) = \sigma_{ho}(\varepsilon) + \sigma_{rubber}(\varepsilon)\cdot\bar{\rho}_i \sin^2\omega \tag{7}$$

Consequently, the energy absorption capacity per unit volume of a hybrid truss CPL structure can be expressed as $W_v = \int_0^{\varepsilon_D}[\sigma_{ho}(\varepsilon) + \sigma_{rubber}(\varepsilon)\cdot\bar{\rho}_i \sin^2\omega]d\varepsilon$. Because of the super-elasticity of silicone rubber, we expect that the energy absorption capacity per unit volume will be increased compared with that of a hollow truss CPL structure without rubber cores. The corresponding energy absorption per unit mass W_m is given by $W_m = W_v/(\bar{\rho}\rho_{cf})$, then one can predict that the energy absorption per unit mass of hybrid truss CPL structure will surpass that of hollow truss counterpart when

$$\int_0^{\varepsilon_D}\sigma_{rubber}(\varepsilon)d\varepsilon > \frac{1}{\bar{\rho}_{cf}\sin^2\omega}\int_0^{\varepsilon_D}\sigma_{ho}(\varepsilon)d\varepsilon \tag{8}$$

Because the left side of the inequality (8) is a constant after the rubber is selected, hollow truss CPL structures can be designed to satisfy the inequality (8). By so doing, the energy absorption of their corresponding hybrid truss CPL structures (both per unit volume and mass) can be increased. Thus, employing the hybrid truss construction, we can provide a route to introduce additional functionality to lattice structures without compromising their intrinsic compressive properties.

The energy absorption of CPL structures with rubber–core trusses (Type A) and hollow trusses is summarized in Fig. 8, together with the experimental data for hollow truss CPL structures [14] and comparing with the reported good candidates of metallic lattice [23]. The energy absorption values per unit volume of rubber–core truss CPL structures are greater than those of hollow truss CPL structures, although the corresponding energy absorption per unit mass is much lower in the present study.

4.3.1. Effect of failure mode

Note that the energy absorption capability demonstrated here is affected by the failure mode of the rubber–core trusses. As shown in Fig. 6b, the CPL structures with circumferentially stacked unidirectional prepreg failed by tube wall fracture in the present study. Note that the failure mode here is similar to that hollow truss CPL involving woven composites [14]. Only because the rubber is constrained circumferentially and does not buckle with progressive loading, does the stress continue to increase. A trial CPL was produced with only 0 fibers (uniaxially lying along the truss

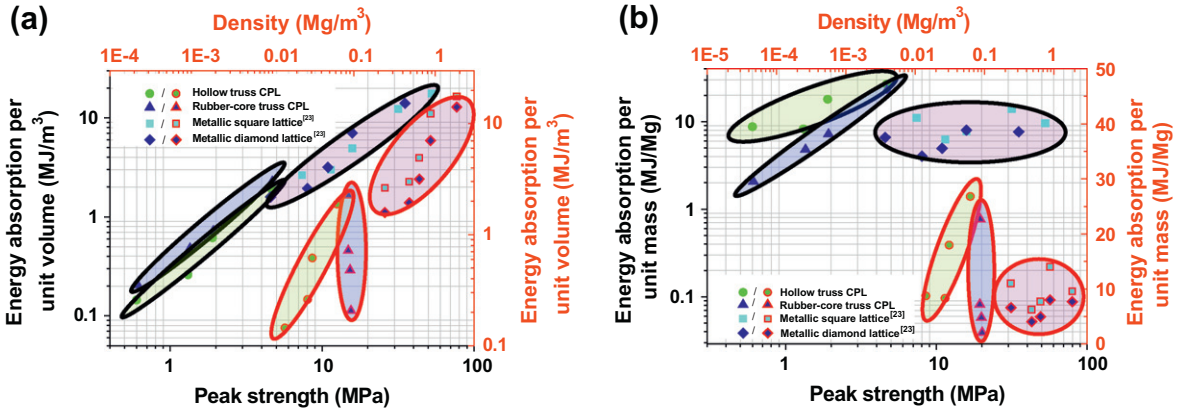

Fig. 8. Energy absorption (a) per unit volume (b) per unit mass of composite pyramidal lattice structures with rubber–core trusses compared with those of the corresponding hollow truss counterparts.

member) to illustrate this point and Fig. 6c shows the failure mode of this structure. The circumferential arrangement of fibers is important to constrain the rubber core and ensure the fracture of the composite tube.

4.3.2. Core–shell proportions

For CPL structures with a fixed pyramidal core geometry, as the rubber core diameter d_i decreases, the relative density occupied by the carbon fiber composites $\bar{\rho}_{cf}$ will increase and the peak strength of hollow truss lattice structures will increase as well [14]. Accordingly, the corresponding energy absorption capacity of hybrid truss CPL structures will increase. However, as the relative density occupied by the incorporated rubber $\bar{\rho}_i$ decreases, the energy absorption proportion contributed by silicone rubber will decrease.

5. Conclusions

A hybrid truss construction has been developed for CF CPL sandwich structures with the objective of demonstrating a strengthening strategy for traditionally ultra-lightweight solid truss CPL structures, while simultaneously introducing additional functionality into the trusses. Wood and silicone rubber were chosen as the embedded core materials for the two objectives, respectively.

Out-of-plane compression tests were carried out to evaluate the properties. The compressive response revealed that the embedded core did not affect the initial (typically linear) response characteristics of CF CPL sandwich structures, an observation explained by the much greater strength of carbon fiber composites compared to the embedded wood/rubber. The specific properties depended on the diameter and density of the core materials. In the present study, the specific strength of wood–core truss CPL increased by >19%, while that of rubber–core CPL decreased compared to that of the solid truss CPL structures. However, specific strength analysis showed that either of the two core materials can be used to increase the structural efficiency if the diameter is appropriately selected. Although the specific strength of the hollow truss is the greatest (Table 2) due to the absence of the weight penalty of the embedded core, the energy absorption capability of rubber–core truss CPL structures increased relative to the counterpart hollow truss CPL structures. Thus, we conclude that the multifunctionality of CPL structures can be achieved by adding function into the hollow truss cavity without compromising compressive properties or increasing fabrication difficulty. The governing failure mode of these newly developed constructions was tube wall fracture of hybrid trusses. This is significant, since ultra-lightweight lattice cores typically failed by Euler buckling of trusses [15,16].

The hybrid truss construction employed here provides a pathway to design lattice structures with increased density-specific performance and multifunctional characteristics by judicious selection of embedded core materials and geometries. The construction concept is equally applicable to pyramidal lattice structures and other topologies. Wood and silicone rubber core materials were selected here to demonstrate the hybrid truss concept, although other materials can be selected for specific ranges of applicability and functions. The hybrid approach and the simple fabrication techniques afford opportunity to incorporate different functions into such structures, increasing the potential for designing a wide range of multifunctional structures. Realization of this potential awaits future research efforts in this vein.

Acknowledgements

The present work is supported by NSFC (90816024 and 10872059), 973 Program (No. 2011CB610303), Program for NCET (NCET-08-0152) and Program of Excellent Team in HIT and the Fundamental Research Funds for the Central Universities (Grant No. HIT. KLOF2010029). S.N. gratefully acknowledges support from the Gill Composites Center. S.Y. also acknowledges the support of Most Potential New Scholar Prize awarded by Ministry of Education in China (AUDQ1010000511).

References

[1] Evans AG, Hutchinson JW, Fleck NA, Ashby MF, Wadley HNG. The topological design of multifunctional cellular metals. Prog Mater Sci 2001;46(3–4):309–27.
[2] Wadley HNG. Multifunctional periodic cellular metals. Philos Trans R Soc A – Math Phys Eng Sci 2006;364(1838):31–68.
[3] Lu TJ, Valdevit L, Evans AG. Active cooling by metallic sandwich structures with periodic cores. Prog Mater Sci 2005;50(7):789–815.
[4] Lu TJ, Stone HA, Ashby MF. Heat transfer in open-cell metal foams. Acta Mater 1998;46(10):3619–35.
[5] Yungwirth CJ, Radford DD, Aronson M, Wadley HNG. Experiment assessment of the ballistic response of composite pyramidal lattice truss structures. Compos Part B – Eng 2008;39(3):556–69.
[6] Ashby MF, Brechet YJM. Designing hybrid materials. Acta Mater 2003;51(19):5801–21.
[7] Deshpande VS, Fleck NA, Ashby MF. Effective properties of the octet-truss lattice material. J Mech Phys Solids 2001;49(8):1747–69.
[8] Lee YH, Lee BK, Jeon I, Kang KJ. Wire-woven bulk Kagome truss cores. Acta Mater 2007;55(18):6084–94.
[9] Queheillalt DT, Murty Y, Wadley HNG. Mechanical properties of an extruded pyramidal lattice truss sandwich structure. Scripta Mater 2008;58(1):76–9.
[10] Jacobsen AJ, Barvosa-Carter W, Nutt S. Compression behavior of micro-scale truss structures formed from self-propagating polymer waveguides. Acta Mater 2007;55(20):6724–33.
[11] Jacobsen AJ, Barvosa-Carter W, Nutt S. Micro-scale truss structures with three-fold and six-fold symmetry formed from self-propagating polymer waveguides. Acta Mater 2008;56(11):2540–8.
[12] Bouwhuis BA, Ronis T, McCrea JL, Palumbo G, Hibbard GD. Structural nanocrystalline Ni coatings on periodic cellular steel. Compos Sci Technol 2009;69(3–4):385–90.
[13] Finnegan K, Kooistra G, Wadley HNG, Deshpande VS. The compressive response of carbon fiber composite pyramidal truss sandwich cores. Int J Mater Res 2007;98(12):1264–72.
[14] Yin S, Wu LZ, Ma L, Nutt S. Pyramidal lattice sandwich structures with hollow composite trusses. Compos Struct 2011. doi:10.1016/j.compstruct.2011.06.02.
[15] Wang B, Wu LZ, Ma L, Sun YG, Du SY. Mechanical behavior of the sandwich structures with carbon fiber-reinforced pyramidal lattice truss core. Mater Des 2010;31(5):2659–63.
[16] Xiong J, Ma L, Wu L, Wang B, Vaziri A. Fabrication and crushing behavior of low density carbon fiber composite pyramidal truss structures. Compos Struct 2010;92(11):2695–702.
[17] Fan HL, Meng FH, Yang W. Sandwich panels with Kagome lattice cores reinforced by carbon fibers. Compos Struct 2007;81(4):533–6399.
[18] Fan HL, Fang DN, Chen LM, Dai Z, Yang W. Manufacturing and testing of a CFRC sandwich cylinder with Kagome cores. Compos Sci Technol 2009;69(15–16):2695–700.
[19] Fan HL, Yang W, Zhou Q. Experimental research of compressive responses of multi-layered woven textile sandwich panels under quasi-static loading. Compos Part B – Eng 2011;42(5):1151–6.
[20] ASTM: C365/C 364M-05. Standard test method for flat wise compressive properties of sandwich cores. Weat Conshohocken (PA): ASTM Int.; 2006.
[21] Budiansky B. On the minimum weights of compression structures. Int J Solids Struct 1999;36(24):3677–708.
[22] Ashby MF et al. Metal foams: a design guide. Woburn: Butterworth-Heinemann; 2000.
[23] Queheillalt DT, Wadley HNG. Cellular metal lattices with hollow trusses. Acta Mater 2005;53(2):303–13.